Original article

MOLECULAR METABOLISM

GLP-2 receptor signaling controls circulating bile acid levels but not glucose homeostasis in *Gcgr*$^{-/-}$ mice and is dispensable for the metabolic benefits ensuing after vertical sleeve gastrectomy

Anita Patel [1,2,6], **Bernardo Yusta** [5,6], **Dianne Matthews** [5], **Maureen J. Charron** [3,4], **Randy J. Seeley** [2], **Daniel J. Drucker** [5,*]

ABSTRACT

Objective: Therapeutic interventions that improve glucose homeostasis such as attenuation of glucagon receptor (Gcgr) signaling and bariatric surgery share common metabolic features conserved in mice and humans. These include increased circulating levels of bile acids (BA) and the proglucagon-derived peptides (PGDPs), GLP-1 and GLP-2. Whether BA acting through TGR5 (Gpbar1) increases PGDP levels in these scenarios has not been examined. Furthermore, although the importance of GLP-1 action has been interrogated in *Gcgr*$^{-/-}$ mice and after bariatric surgery, whether GLP-2 contributes to the metabolic benefits of these interventions is not known.

Methods: To assess whether BA acting through Gpbar1 mediates improved glucose homeostasis in *Gcgr*$^{-/-}$ mice we generated and characterized *Gcgr*$^{-/-}$:*Gpbar1*$^{-/-}$ mice. The contribution of GLP-2 receptor (GLP-2R) signaling to intestinal and metabolic adaptation arising following loss of the Gcgr was studied in *Gcgr*$^{-/-}$:*Glp2r*$^{-/-}$ mice. The role of the GLP-2R in the metabolic improvements evident after bariatric surgery was studied in high fat-fed *Glp2r*$^{-/-}$ mice subjected to vertical sleeve gastrectomy (VSG).

Results: Circulating levels of BA were markedly elevated yet similar in *Gcgr*$^{-/-}$:*Gpbar1*$^{+/+}$ vs. *Gcgr*$^{-/-}$:*Gpbar1*$^{-/-}$ mice. Loss of GLP-2R lowered levels of BA in *Gcgr*$^{-/-}$ mice. *Gcgr*$^{-/-}$:*Glp2r*$^{-/-}$ mice also exhibited shifts in the proportion of circulating BA species. Loss of *Gpbar1* did not impact body weight, intestinal mass, or glucose homeostasis in *Gcgr*$^{-/-}$ mice. In contrast, small bowel growth was attenuated in *Gcgr*$^{-/-}$:*Glp2r*$^{-/-}$ mice. The improvement in glucose tolerance, elevated circulating levels of GLP-1, and glucose-stimulated insulin levels were not different in *Gcgr*$^{-/-}$:*Glp2r*$^{+/+}$ vs. *Gcgr*$^{-/-}$:*Glp2r*$^{-/-}$ mice. Similarly, loss of the GLP-2R did not attenuate the extent of weight loss and improvement in glucose control after VSG.

Conclusions: These findings reveal that GLP-2R controls BA levels and relative proportions of BA species in *Gcgr*$^{-/-}$ mice. Nevertheless, the GLP-2R is not essential for i) control of body weight or glucose homeostasis in *Gcgr*$^{-/-}$ mice or ii) metabolic improvements arising after VSG in high fat-fed mice. Furthermore, despite elevations of circulating levels of BA, Gpbar1 does not mediate elevated levels of PGDPs or major metabolic phenotypes in *Gcgr*$^{-/-}$ mice. Collectively these findings refine our understanding of the relationship between Gpbar1, elevated levels of BA, PGDPs, and the GLP-2R in amelioration of metabolic derangements arising following loss of Gcgr signaling or after vertical sleeve gastrectomy.

Keywords Glucagon; GLP-1; GLP-2; Bile acids; Bariatric surgery; Glucose; Diabetes; Obesity

1. INTRODUCTION

Although multiple organ systems contribute to control of energy balance, the complex network of enteroendocrine cells has received increasing attention as physiological regulators of metabolic homeostasis [1,2]. Notably, L cells that produce the proglucagon-derived peptides (PGDPs) have been extensively studied, as PGDPs exert pleiotropic actions regulating appetite, gastrointestinal motility,

[1]Neuroscience Graduate Program, University of Michigan, Ann Arbor, MI, USA [2]Department of Surgery, Internal Medicine and Nutritional Science, University of Michigan, Ann Arbor, MI, USA [3]Department of Biochemistry, Medicine (Endocrinology), Albert Einstein College of Medicine, USA [4]Department of Obstetrics & Gynecology and Women's Health, Albert Einstein College of Medicine, USA [5]Department of Medicine, Lunenfeld-Tanenbaum Research Institute, Mt. Sinai Hospital, University of Toronto, Ontario, M5G 1X5, Canada

[6] AP and BY are co-first authors.

*Corresponding author. Lunenfeld-Tanenbaum Research Institute, Mt. Sinai Hospital, 600 University Ave Mailbox 39, TCP5-1004, Toronto, ON, M5G 1X5, Canada. E-mail: drucker@lunenfeld.ca (D.J. Drucker).

Received May 17, 2018 • Revision received June 4, 2018 • Accepted June 6, 2018 • Available online 9 June 2018

https://doi.org/10.1016/j.molmet.2018.06.006

nutrient absorption, gut epithelial integrity, gallbladder emptying, and the uptake and assimilation of nutrients in peripheral tissues [3,4]. Indeed, PGDP secretion from enteroendocrine L cells is stimulated by a range of nutrients, microbial metabolites, and bile acids (BA), through direct and indirect mechanisms [2].

Glucagon-like peptide-1 (GLP-1), the best characterized PGDP, is a 30 amino acid peptide that exerts its actions through a single well-defined G protein-coupled receptor [4]. GLP-1 is physiologically essential for glucose control and energy homeostasis, as revealed in preclinical studies using GLP-1 receptor (GLP-1R) antagonists or *Glp1r*$^{-/-}$ mice [4]. GLP-1 also attenuates the rate of gastric emptying and small bowel motility, and promotes expansion of the intestinal mucosal epithelium, actions serving to optimize the efficiency of nutrient absorption [5]. Although less well studied, the related PGDP GLP-2 also controls the absorption of nutrients through reduction of gut motility, upregulation of nutrient transport and via optimization of mucosal surface area and gut integrity [6].

A number of experimental therapeutic manipulations resulting in improvement of glucose metabolism and either resistance to weight gain or development of weight loss are characterized by simultaneous elevation of circulating BA and PGDPs. Thus, partial or complete blockade of glucagon action, achieved through genetic loss of hepatic glucagon receptor (*Gcgr*) expression or pharmacological antagonism of GCGR signaling, is associated with a rapid rise in circulating levels of GLP-1 and GLP-2 [7,8]. Unexpectedly, reduction of Gcgr signaling is also associated with markedly increased circulating levels of BA [9,10]. Indeed plasma levels of PGDPs and BA are increased in humans with T2D following daily or chronic administration of GCGR antagonists [8,11].

Bariatric surgery represents a second therapeutic paradigm characterized by increased levels of circulating BA, GLP-1 and GLP-2. Both vertical sleeve gastrectomy (VSG) and Roux-en-Y gastric bypass (RYGB), when performed experimentally in animals, or therapeutically in humans, lead to elevated levels of BA and PGDPs [12–16]. Although BA are known stimulators of L cell PGDP secretion via signaling through TGR5 (Gpbar1) [17–19], the extent if any, to which elevated levels and action of BA contribute to increased levels of circulating PGDPs i) in animals or humans with loss of GCGR action or ii) following bariatric surgery, has not been yet determined.

The finding that enhanced circulating levels of BA and PGDPs are simultaneously associated with improved glucose control in the setting of loss of GCGR signaling or metabolic surgery raises important mechanistic questions [20–22]. Notably, preclinical studies implicate a role for BA, acting through changes in the gut microbiota and via the nuclear Farnesoid X Receptor (FXR), in the improvements in glucose control and weight loss ensuing following VSG [23]. Consistent with the importance of BA in this setting, the metabolic benefits ensuing from bariatric surgery are also attenuated in *Gpbar1*$^{-/-}$ mice [24,25]. Although somewhat controversial, GLP-1 contributes to improvements in β-cell function in some [26], but not all murine studies of metabolic surgery [20,27]. It seems likely that GLP-1 improves β-cell function in humans after bariatric surgery, and in rare instances, promotes development of hyperinsulinemic hypoglycemia [21].

In contrast to the extensive literature describing the metabolic roles of GLP-1, much less is known about the effects of GLP-2 on glucose control and body weight. Notably, GLP-2 inhibits ghrelin secretion [28], enhances hepatic insulin sensitivity [29], and suppresses food intake [30], actions mirroring some of the metabolic benefits ensuing after bariatric surgery or GCGR antagonism. Furthermore, GLP-2 enhances gut adaptation and barrier function while reducing metabolic endotoxemia [6,31], consistent with intestinal adaptation evident after VSG or RYGB [32,33]. Collectively, these observations raise the possibility that elevated levels of GLP-2, arising secondarily to or independent from increased levels of BA, may contribute to the metabolic benefits arising following i) reduction of GCGR signaling or ii) metabolic surgery. To interrogate the potential role of BA signaling through Gpbar1 and the importance of GLP-2R for the metabolic improvements in *Gcgr*$^{-/-}$ mice, we generated *Gcgr*$^{-/-}$:*Gpbar1*$^{-/-}$ and *Gcgr*$^{-/-}$:*Glp2r*$^{-/-}$ mice. Simultaneously, we examined the importance of GLP-2R signaling in *Glp2r*$^{-/-}$ mice following experimental VSG.

2. MATERIALS AND METHODS

2.1. Animals and vertical sleeve gastrectomy surgical procedure

Gcgr$^{-/-}$ mice provided by Maureen Charron [34], *Tgr5*$^{-/-}$ (*Gpbar1*$^{-/-}$) mice [35], obtained from Schering-Plough/Merck, and *Glp2r*$^{-/-}$ mice [36], all on a C57Bl/6 background were bred at the Toronto Centre for Phenogenomics animal facility. *Gcgr*$^{-/-}$:*Gpbar1*$^{-/-}$ and *Gcgr*$^{-/-}$:*Glp2r*$^{-/-}$ double knockout mice were generated by crossing double heterozygous *Gcgr*$^{+/-}$:*Gpbar1*$^{+/-}$ *or* *Gcgr*$^{+/-}$:*Glp2r*$^{+/-}$ to obtain wild-type, single knockout and double knockout littermates. All experiments involving *Gcgr*$^{-/-}$:*Gpbar1*$^{-/-}$ and *Gcgr*$^{-/-}$:*Glp2r*$^{-/-}$ double knockout mice and their single knockout and wild-type littermates were performed in male aged 12–26 weeks, housed up to 5 per cage, with free access to food (2018 Teklad global, Envigo Corp, Mississauga, ON, Canada) and water. VSG or sham surgeries were performed on male *Glp2r*$^{-/-}$ and wild-type littermate mice bred in-house at the University of Michigan. Four to 11 week old mice were placed on a 60% high fat diet (HFD) (D12492, Research Diets, New Brunswick, NJ, USA) were single housed and given ad libitum access to food. After 8 weeks, surgeries were performed as previously described [37]. Briefly, while mice were anesthetized under isoflurane inhalation, an abdominal midline laparotomy was made followed by incision of the underlying abdominal muscle and exteriorization of the stomach. For VSG the lateral 80% of the stomach was excised using an ETS 35-mm staple gun (Ethicon Endo-Surgery, Cincinnati, OH, USA) leaving a tubular gastric sleeve in continuity with the esophagus proximally and the pylorus distally. The sham procedure involved the application of light pressure on the stomach with blunt forceps. Mice were fed Osmolite 1.0 Cal liquid diet (Abbott Nutrition, Lake Forest, IL, USA) from 1 day prior to surgery to 3 days following surgery before returning to 60% HFD. *Glp2r*$^{-/-}$ pair-fed animals underwent sham surgery and were restricted to eating the daily average amount of food eaten by the *Glp2r*$^{-/-}$ mice subjected to VSG. Pair-feeding continued until sacrifice. Body composition was measured using an EchoMRI (Echo Medical Systems, Houston, TX, USA) 1 week prior to surgery and 6 and 8 weeks after surgery. Body weights were measured daily for 1 week after surgery and weekly for 10 weeks thereafter. All animal experiments performed in Toronto were conducted according to protocols approved by the Animal Care and Use Subcommittee at the Toronto Centre for Phenogenomics, Mt. Sinai Hospital, and were consistent with the ARRIVE guidelines. Studies on *Glp2r*$^{-/-}$ mice done in Ann Arbor were approved by the Institutional Animal Care & Use Committee at the University of Michigan (Animal Use Protocol #PRO00005678).

2.2. Glucose tolerance tests and measurement of plasma insulin, GLP-1 and bile acids

Glucose tolerance tests in *Gcgr*$^{-/-}$:*Gpbar1*$^{-/-}$ and *Gcgr*$^{-/-}$:*Glp2r*$^{-/-}$ double knockout mice and their single knockout and wild-type littermates were carried out in 12- to 15-week-old mice. Fed or overnight fasted (16–18 h in cages with wire grid flooring) mice were administered glucose (2 mg/g body weight) via either an oral gavage or i.p.

injection. Glycemic excursion curves were delineated by measuring tail blood glycemia using a Contour blood glucose meter (Bayer Inc, Mississauga, ON, Canada) at 0, 15, 30 60 and 90 min after glucose loading. Glucose tolerance tests in *Glp2r*$^{-/-}$ and wild-type littermate mice that underwent VSG or SH surgeries were performed during postoperative week 5 following a 4 h fasting after the onset of light. Baseline blood glucose was measured in tail blood using an Accu-Check glucometer (Roche Diabetes Care, Mannheim, Germany) 30 min prior to i.p. injection of 2 mg glucose/g body weight or oral gavage of 2.6 mg glucose/g body weight. Tail blood glucose was measured at 15, 30, 45, 60, and 120 min following glucose administration. For plasma BA measurement, blood samples were collected from the tail vein into heparin-coated tubes (Sarstedt, Montreal, QC, Canada). For plasma insulin and GLP-1 determination, blood samples collected into heparin-coated tubes, were supplemented with 1/10 the blood volume of a solution containing 5000 KIU/ml Trasylol (Bayer Inc, Mississauga, ON, Canada), 32 mM EDTA, and 0.01 mM Diprotin A (Sigma, St. Louis, MO, USA). Plasma was separated by centrifugation at 4 °C and stored at −80 °C until assayed for insulin (ultrasensitive mouse insulin ELISA; Alpco Diagnostics, Salem, NH, USA) and GLP-1 (mouse/rat total GLP-1 assay kit; Mesoscale Discovery, Gaithersburg, MD, USA). GLP-1, but not GLP-2, was measured as a readout of L cell secretion since the commercially available GLP-2 assays have not been sufficiently validated to ensure accurate measurement of total or intact GLP-2 [6]. Total bile acid levels in plasma were quantified using an assay kit based in the colorimetric detection of thio-NADH generated following oxidation of the bile acids by the enzyme 3-alpha-hydroxysteroid dehydrogenase in the presence of excess NADH (Diazyme Laboratories, Poway, CA, USA).

2.3. Intestinal biometry

Following euthanasia, mice were weighed and tibial length measured with a caliper. The entire gastrointestinal tract from the stomach to the rectum was removed, cleaned of mesenteric fat and gut weight and length determined. Small intestine length was measured under tension by suspending a 1-g weight from the distal end, prior to flushing with PBS to remove luminal content, whereas colon length was measured on a horizontal ruler after flushing. The entire small bowel and colon were then blotted to remove PBS before being weighed.

2.4. RNA isolation and analysis of mRNA expression

Total RNA from mouse ileum and liver was extracted by the guanidinium thiocyanate method using TRI Reagent (Molecular Research Center Inc, Cincinnati, OH, USA). Reverse transcription was performed with 500 ng of total RNA treated with DNase I (#EN0521, Thermo-Fisher Scientific, Markham ON, Canada), using random hexamers (#58875) and SuperScript III (#18080-044) from Thermo-Fisher Scientific. The resultant cDNA was used to assess mRNA expression by real-time quantitative PCR (QuantStudio 5 System, Thermo-Fisher Scientific) with TaqMan Fast Advanced Master Mix (#4444557, Thermo-Fisher Scientific) and TaqMan Gene Expression Assays (Thermo-Fisher Scientific). The specific gene expression assays used are listed in Supplementary Table 1. Quantification of transcript levels was performed by the $2^{-\Delta Ct}$ method using 18S rRNA or *Ppia* for normalization.

2.5. Quantitative profiling of bile acids from ileum and plasma

Samples of plasma and ileum (with associated luminal content) from random-fed *Gcgr*$^{-/-}$*:Glp2r*$^{-/-}$ double knockout mice and their single knockout and wild-type littermates, were analyzed by the Michigan Regional Comprehensive Metabolomics Resource (MRC2) facility using a modified protocol as previously described [38]. Serum and ileum samples underwent a two-step solvent extraction as follows. Samples were mixed with 100% ethanol with isotope-labeled internal standards and homogenized using a probe sonication. Samples rested on ice for 10 min and subsequently vortexed. An aliquot of this sample was transferred to a new glass tube and centrifuged. Supernatant was transferred to a microtube. An 8:1:1 solution of methanol, chloroform, and water was mixed to the glass tube and rested for 10 min followed by centrifugation. Supernatants were collected and combined. Samples were then dried at 45 °C using a vacuum centrifuge for 45min and reconstituted in 50% methanol in water solution.

LC-MS analysis: LC-MS analysis was performed on an Agilent system consisting of a 1290 UPLC module coupled with a 6490 Triple Quad (QqQ) mass spectrometer (Agilent Technologies, Santa Clara, CA) operated in MRM mode. Metabolites were separated on a 100 mm × 2.1 mm Acquity BEH UPLC (1.7 uM) column (Waters Corp, Milford, MA) using H_2O, 0.1% Formic acid, as mobile phase A, and Acetonitrile, 0.1% Formic acid, as mobile phase B. The flow rate was

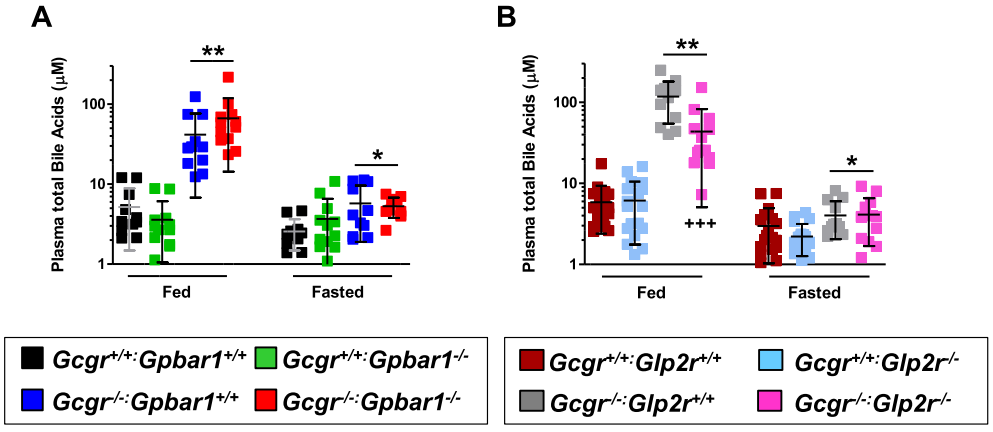

Figure 1: Plasma total bile acid levels in *Gcgr*$^{-/-}$*:Gpbar1*$^{-/-}$ (A) and *Gcgr*$^{-/-}$*:Glp2r*$^{-/-}$ (B) double knockout mice and their single knockout and wild-type littermates. Shown are individual data points with overlapping mean ± SD (n = 11–16 mice per genotype, combined from 2 independent mouse cohorts). Panel A: *p < 0.05 & **p < 0.01 *Gcgr*$^{-/-}$*:Gpbar1*$^{+/+}$ & *Gcgr*$^{-/-}$*:Gpbar1*$^{-/-}$ vs *Gcgr*$^{+/+}$*:Gpbar1*$^{+/+}$& *Gcgr*$^{+/+}$*:Gpbar1*$^{-/-}$. Panel B: *p < 0.05 *Gcgr*$^{-/-}$*:Glp2r*$^{+/+}$ & *Gcgr*$^{-/-}$*:Glp2r*$^{-/-}$ vs *Gcgr*$^{+/+}$*:Glp2r*$^{-/-}$; **p < 0.01 *Gcgr*$^{-/-}$*:Glp2r*$^{+/+}$ & *Gcgr*$^{-/-}$*:Glp2r*$^{-/-}$ vs *Gcgr*$^{+/+}$*:Glp2r*$^{+/+}$ & *Gcgr*$^{+/+}$*:Glp2r*$^{-/-}$; +++p < 0.001 *Gcgr*$^{-/-}$*:Glp2r*$^{-/-}$ vs *Gcgr*$^{-/-}$*:Glp2r*$^{+/+}$. Statistical significance was assessed by one-way ANOVA followed by Bonferroni's multiple comparison post hoc test.

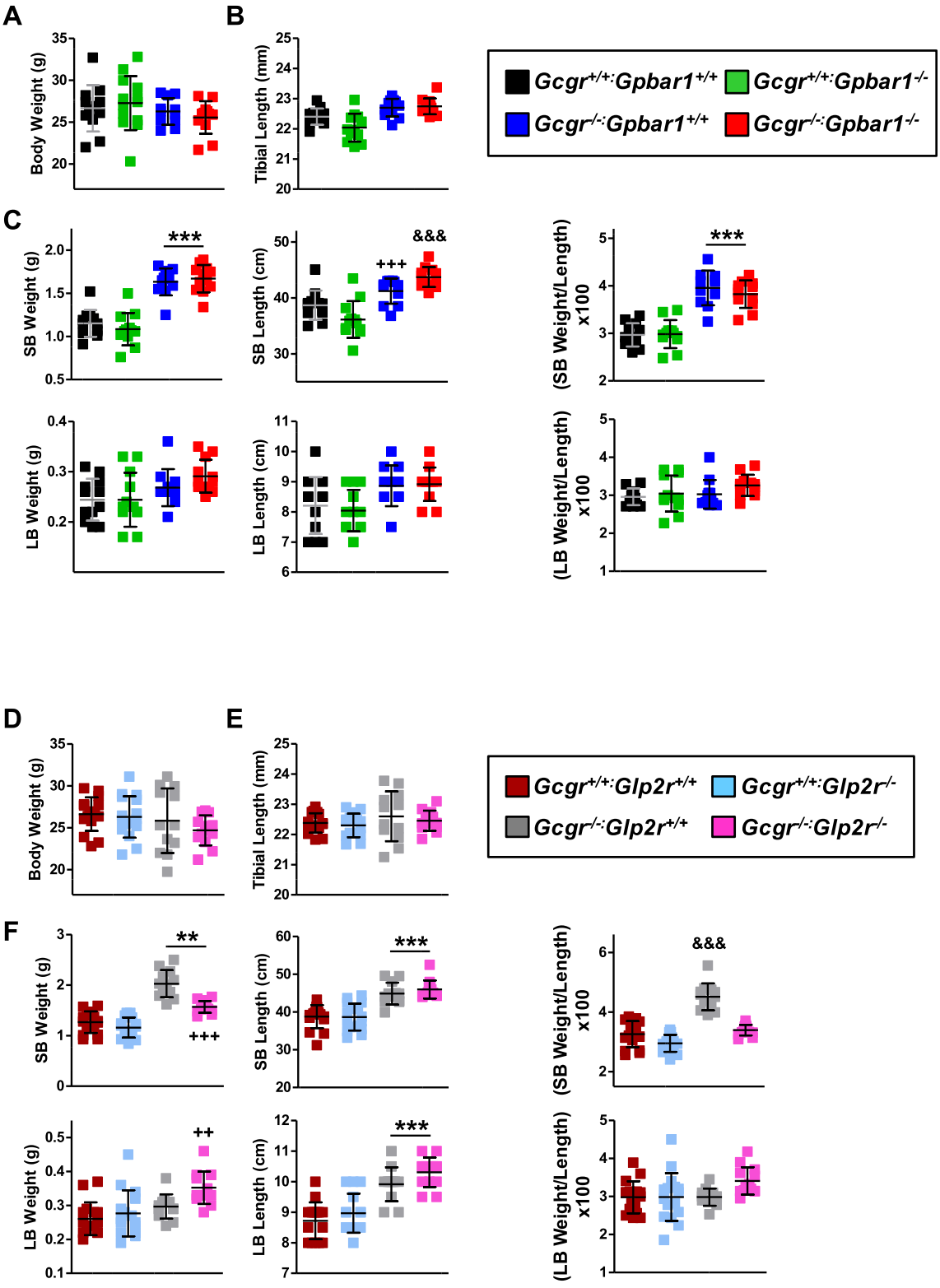

Figure 2: Body weight (A & D), tibial length (B & E) and intestinal biometry (C & F) in *Gcgr*$^{-/-}$:*Gpbar1*$^{-/-}$ (A–C) and *Gcgr*$^{-/-}$:*Glp2r*$^{-/-}$ (D–F) double knockout mice and their single knockout and wild-type littermates. Body weight was assessed following overnight fasting 1 week before take down which was performed under random-fed conditions. Shown are individual data points with overlapping mean ± SD (n = 11–16 mice per genotype, combined from 2 independent mouse cohorts). SB: small bowel, LB: large bowel. Panel C: ***p < 0.001 *Gcgr*$^{-/-}$:*Gpbar1*$^{+/+}$ & *Gcgr*$^{-/-}$:*Gpbar1*$^{-/-}$ vs *Gcgr*$^{+/+}$:*Gpbar1*$^{+/+}$ & *Gcgr*$^{+/+}$:*Gpbar1*$^{-/-}$; +++p < 0.001 *Gcgr*$^{-/-}$:*Gpbar1*$^{+/+}$ vs *Gcgr*$^{+/+}$:*Gpbar1*$^{-/-}$; &&&p < 0.001 *Gcgr*$^{-/-}$:*Gpbar1*$^{-/-}$ vs *Gcgr*$^{+/+}$:*Gpbar1*$^{+/+}$ & *Gcgr*$^{+/+}$:*Gpbar1*$^{-/-}$. Panel F: **p < 0.01 & ***p < 0.001 *Gcgr*$^{-/-}$:*Glp2r*$^{+/+}$ & *Gcgr*$^{-/-}$:*Glp2r*$^{-/-}$ vs *Gcgr*$^{+/+}$:*Glp2r*$^{+/+}$ & *Gcgr*$^{+/+}$:*Glp2r*$^{-/-}$; ++p < 0.01 *Gcgr*$^{-/-}$:*Glp2r*$^{-/-}$ vs *Gcgr*$^{+/+}$:*Glp2r*$^{+/+}$ & *Gcgr*$^{+/+}$:*Glp2r*$^{-/-}$; +++p < 0.001 *Gcgr*$^{-/-}$:*Glp2r*$^{-/-}$ vs *Gcgr*$^{-/-}$:*Glp2r*$^{+/+}$; &&&p < 0.001 *Gcgr*$^{-/-}$:*Glp2r*$^{+/+}$ vs *Gcgr*$^{+/+}$:*Glp2r*$^{+/+}$, *Gcgr*$^{+/+}$:*Glp2r*$^{-/-}$ & *Gcgr*$^{-/-}$:*Glp2r*$^{-/-}$. Statistical significance was assessed by one-way ANOVA followed by Bonferroni's multiple comparison post hoc test.

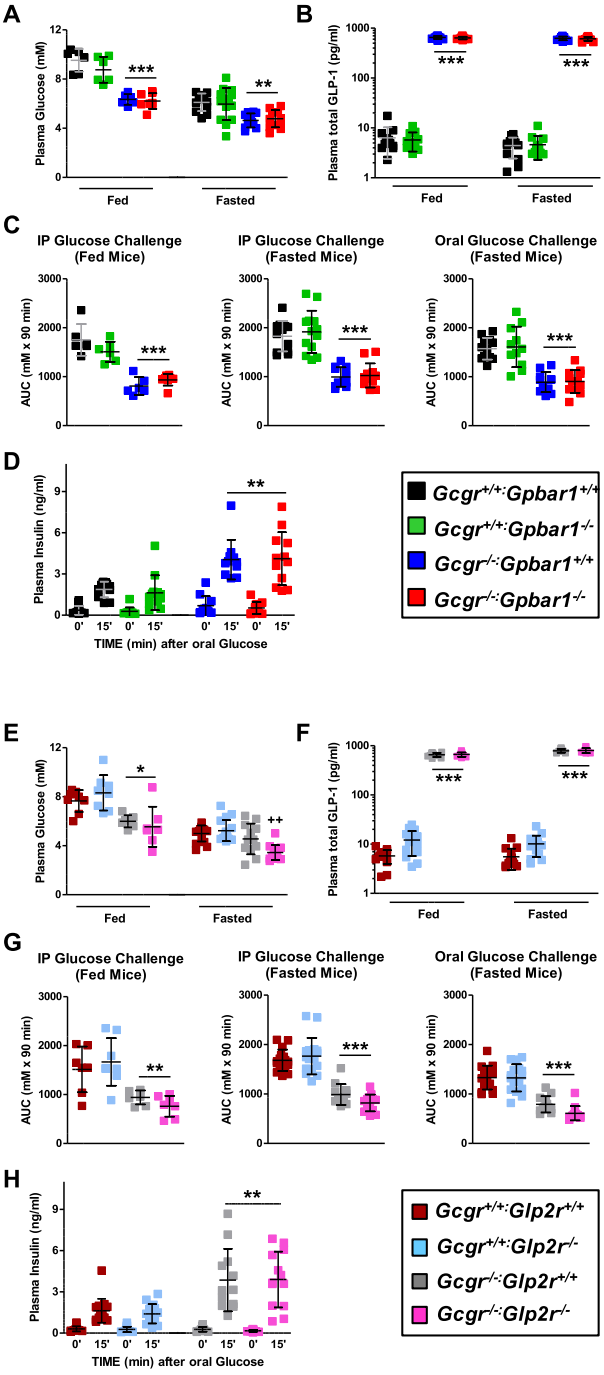

Figure 3: Fasting and fed glycemia (A & E) and plasma total GLP-1 (B & F), area under the glycemic excursion curves (AUC) (C & G) and plasma insulin at 0 and 15 min after oral glucose challenge in *Gcgr*$^{-/-}$:*Gpbar1*$^{-/-}$ (A–D) and *Gcgr*$^{-/-}$:*Glp2r*$^{-/-}$ (E–H) double knockout mice and their single knockout and wild-type littermates. Glycemic excursion curves were delineated by measuring tail blood glycemia at 0, 15, 30 60 and 90 min after the specified glucose challenge and glucose tolerance determined by calculating the corresponding AUCs. Shown are individual data points with overlapping mean ± SD (n = 11–16 mice per genotype, combined from 2 independent mouse cohorts, except data from fed mice in panels A, C, E and G wherein n = 6–8 per genotype). Panels A, B & C: **p < 0.01 & ***p < 0.001 *Gcgr*$^{-/-}$:*Gpbar1*$^{+/+}$ & *Gcgr*$^{-/-}$:*Gpbar1*$^{-/-}$ vs *Gcgr*$^{+/+}$:*Gpbar1*$^{+/+}$ & *Gcgr*$^{+/+}$:*Gpbar1*$^{-/-}$. Panels E, F, & G: *p < 0.05, **p < 0.01 & ***p < 0.001 *Gcgr*$^{-/-}$:*Glp2r*$^{+/+}$ & *Gcgr*$^{-/-}$:*Glp2r*$^{-/-}$ vs *Gcgr*$^{+/+}$:*Glp2r*$^{+/+}$ & *Gcgr*$^{+/+}$:*Glp2r*$^{-/-}$; ++p < 0.01 *Gcgr*$^{-/-}$:*Glp2r*$^{-/-}$ vs *Gcgr*$^{+/+}$:*Glp2r*$^{+/+}$, *Gcgr*$^{+/+}$:*Glp2r*$^{-/-}$ & *Gcgr*$^{-/-}$:*Glp2r*$^{+/+}$. Panels D & H: insulin levels 15 min after oral glucose were significantly higher than at 0 min (p < 0.001) irrespective of the mouse genotype. Panel D: **p < 0.01 *Gcgr*$^{-/-}$:*Gpbar1*$^{+/+}$ & *Gcgr*$^{-/-}$:*Gpbar1*$^{-/-}$ insulin at 15 min vs *Gcgr*$^{+/+}$:*Gpbar1*$^{+/+}$ & *Gcgr*$^{+/+}$:*Gpbar1*$^{-/-}$ insulin at 15 min. Panel H: **p < 0.01 *Gcgr*$^{-/-}$:*Glp2r*$^{+/+}$ & *Gcgr*$^{-/-}$:*Glp2r*$^{-/-}$ insulin at 15 min vs *Gcgr*$^{+/+}$:*Glp2r*$^{+/+}$ & *Gcgr*$^{+/+}$:*Glp2r*$^{-/-}$ insulin at 15 min Statistical significance was assessed by one-way ANOVA followed by Bonferroni's multiple comparison post hoc test. Unpaired Student's t test was used for the comparisons insulin at 15 min vs insulin at 0 min.

0.25 mL/min with the following gradient: linear from 5 to 25% B over 2 min, linear from 25 to 40% B over 14 min, linear from 40 to 95% B over 2 min, followed by isocratic elution at 95% B for 5 min. The system was returned to starting conditions (5% B) in 0.1 min and held there for 3 min to allow for column re-equilibration before injecting another sample. The mass spectrometer was operated in ESI. Data were processed using MassHunter Quantitative analysis version B.07.00. Metabolites were normalized to the nearest isotope labeled internal standard and quantitated using 2 replicated injections of 5 standards to create a linear calibration curve with accuracy better than 80% for each standard.

Bile acid data from ileum were normalized to sample weight prior to processing. Concentrations of GHDA and GUDCA in plasma and CA in ileum are not reported as they were below the detection threshold. (TαMCA + TβMCA), (CDCA + DCA) and (TUDCA + THDCA) indicate sum of concentrations of the indicated pairs of BA which could not be distinguished from each other in the analysis process. Bile acid abbreviations: αMCA (α-Muricholate), βMCA (β-Muricholate), ωMCA (ω-Muricholate), CA (Cholate), CDCA (Chenodeoxycholate), HCA (Hyocholate), DCA (Deoxycholate), UDCA (Ursodeoxycholate), HDCA (Hyodeoxycholate). Taurine (T) conjugated bile acids: TαMCA, TβMCA, TCA, THCA, TCDCA, TDCA, TUDCA, THDCA, TLCA (Taurolithocholate). Glycine (G) conjugated bile acids: GCA, GHCA, GCDCA, GDCA, GUDCA, GHDCA.

2.6. Statistical analysis

Except where indicated, results are presented as scatter plots with overlapping mean ± SD. As specified in the Figure legends, statistical significance was assessed by one-way or two-way ANOVA followed by Bonferroni's multiple comparison post hoc test and, where appropriate, by unpaired Student's t-test. Statistical significance was accepted when $p < 0.05$. All statistical analyses were performed using GraphPad Prism v.7.0 (GraphPad Software, San Diego, CA, USA).

3. RESULTS

As GLP-2 induces the expression of intestinal BA transporters [39] and enhances bile flow [40], we examined whether BAs, acting through *Gpbar1,* or GLP-2, acting through the GLP-2R, contributes to the metabolic phenotypes arising in *Gcgr*$^{-/-}$ mice with markedly increased circulating levels of BA and PGDPs [7,34]. Plasma BA levels were increased in fasted and fed *Gcgr*$^{-/-}$ mice but not significantly different in *Gcgr*$^{-/-}$:*Gpbar1*$^{-/-}$ mice (Figure 1A). In contrast, plasma BA levels remained elevated but were significantly lower in the fed (but not the fasted) state, in *Gcgr*$^{-/-}$:*Glp2r*$^{-/-}$ mice, relative to levels in *Gcgr*$^{-/-}$ *Glp2r*$^{+/+}$ mice (Figure 1B). Hence GLP-2R controls fed state BA levels in *Gcgr*$^{-/-}$ mice.

We next examined the potential roles of *Gpbar1* and *Glp2r* in the intestinal and metabolic phenotypes arising in *Gcgr*$^{-/-}$ mice. Body weight and tibial length were not different in *Gcgr*$^{-/-}$ mice with loss of *Gpbar1* (Figure 2A,B) or *Glp2r* (Figure 2D,E). Small bowel (SB) mass and length was increased in *Gcgr*$^{-/-}$ *Gpbar*$^{+/+}$ mice but not different in *Gcgr*$^{-/-}$:*Gpbar1*$^{-/-}$ mice (Figure 2C), whereas large bowel (LB)

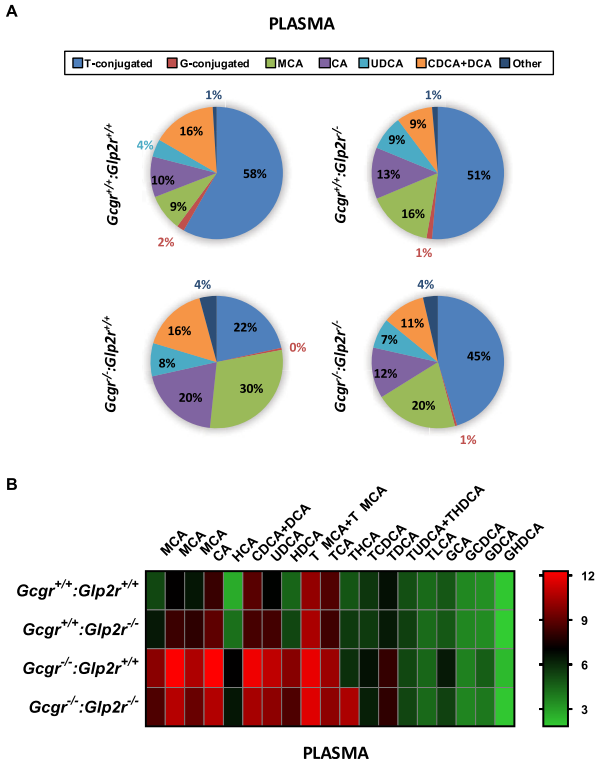

Figure 4: Quantitative profiling of bile acid in plasma from random-fed *Gcgr*$^{-/-}$:*Glp2r*$^{-/-}$ double knockout mice and their single knockout and wild-type littermates. Panel A: Bile acid composition analysis representing the percentage of the major BA which contribute to the BA pool in plasma. Total average concentrations of bile acids in plasma were: *Gcgr*$^{+/+}$:*Glp2r*$^{+/+}$ = 2947.6 nM, *Gcgr*$^{+/+}$:*Glp2r*$^{-/-}$ = 4013.2 nM, *Gcgr*$^{-/-}$:*Glp2r*$^{+/+}$=24942.5 nM and *Gcgr*$^{-/-}$:*Glp2*$^{-/-}$ =13513.9 nM. Panel B: Heat map summarizing the concentrations of the different molecular species of BA quantified in plasma samples. The color code represents the log2 transformation of the corresponding mean BA concentration values. For both Panels A & B n = 8 mice per genotype, combined from 2 independent mouse cohorts. T-conjugated (taurine-conjugated BA), G-conjugated (Glycine-conjugated BA), MCA (sum of αMCA, βMCA and ωMCA concentrations). Scatter plots for the BA illustrated in the heat map are presented in Supplementary Figure 1.

weight and length were similar in *Gcgr*$^{-/-}$:*Gpbar*$^{+/+}$ vs. *Gcgr*$^{-/-}$:*Gpbar1*$^{-/-}$ mice (Figure 2C). SB weight was increased in *Gcgr*$^{-/-}$:*Glp2r*$^{+/+}$ mice but not in *Gcgr*$^{-/-}$:*Glp2r*$^{-/-}$ mice (Figure 2F). In contrast, increases in SB length, as well as LB weight and length were not dependent on the presence or absence of the *Glp2r* (Figure 2F). Hence GLP-2R mediates SB growth in *Gcgr*$^{-/-}$ mice.

Consistent with favorable metabolic phenotypes described in *Gcgr*$^{-/-}$ mice [7,34,41] fasted and fed blood glucose levels were lower and plasma GLP-1 levels were markedly elevated in *Gcgr*$^{-/-}$:*Gpbar1*$^{+/+}$ mice, but not different from levels observed in *Gcgr*$^{-/-}$:*Gpbar1*$^{-/-}$ mice (Figure 3A,B). Similarly, both intraperitoneal and oral glucose tolerance was improved and plasma levels of insulin were increased after glucose challenge in *Gcgr*$^{-/-}$:*Gpbar1*$^{+/+}$ mice, but no differences in these parameters were observed following elimination of *Gpbar1* (Figure 3C,D).

Despite evidence linking *Glp2r* to control of glucose homeostasis and insulin sensitivity in mice [29,30], the presence or absence of the *Glp2r* did not impair the reduction in fed or fasted glycemia, or improvements in glucose tolerance and increases in plasma insulin levels detected in *Gcgr*$^{-/-}$:*Glp2r*$^{+/+}$ vs. *Gcgr*$^{-/-}$:*Glp2r*$^{-/-}$ mice (Figure 3 E,G—H). Furthermore, although levels of fed BA were lower in *Gcgr*$^{-/-}$:*Glp2r*$^{-/-}$ mice, fasted or fed plasma GLP-1 levels measured as a surrogate for the co-secreted PGDP GLP-2, were not different in *Gcgr*$^{-/-}$:*Glp2r*$^{+/+}$ vs. *Gcgr*$^{-/-}$:*Glp2r*$^{-/-}$ mice (Figure 3F).

As plasma BA were lower in fed *Gcgr*$^{-/-}$:*Glp2r*$^{-/-}$ mice (Figure 1B), we next examined the profiles of different BAs in plasma vs. the ileum from *Gcgr*$^{-/-}$:*Glp2r*$^{+/+}$ vs. *Gcgr*$^{-/-}$:*Glp2r*$^{-/-}$ mice. Notably, relative proportions of circulating taurine-conjugated BAs, cholic acid and muricholic acid were increased in *Gcgr*$^{-/-}$:*Glp2r*$^{+/+}$ but were lower in *Gcgr*$^{-/-}$:*Glp2r*$^{-/-}$ mice (Figure 4A,B and Supplementary Figure 1). In contrast, no appreciable differences were detected in proportions of major BA species in the ileum from *Gcgr*$^{-/-}$:*Glp2r*$^{+/+}$ vs. *Gcgr*$^{-/-}$:*Glp2r*$^{-/-}$ mice (Supplementary Figures 2 and 3).

To explore the impact of changes in BA in the same mice, we analyzed the relative expression of a panel of BA-regulated genes in liver and ileum. No consistent genotype-dependent differences were detected in hepatic levels of mRNA transcripts for *Abcc2*, *Abcc3*, *Slc10a1*, *Abcb11*, *Nr1h4*, *Nr0b2*, *Cyp7a1, Cyp8b1* (Figure 5A). In contrast, hepatic mRNA levels of *Slc51b*, encoding the membrane-associated bile acid transporter, were elevated in *Gcgr*$^{-/-}$:*Glp2r*$^{+/+}$ but not in *Gcgr*$^{-/-}$:*Glp2r*$^{-/-}$ mice (Figure 5A). Moreover levels of mRNA transcripts for *Abcc2*, *Abcc3*, *Slc51a*, *Slc51b*, *Nr1h4*, *Fabp6*, and *Fgf15* were not different in ileum RNA from *Gcgr*$^{-/-}$:*Glp2r*$^{+/+}$ vs. *Gcgr*$^{-/-}$:*Glp2r*$^{-/-}$ mice (Figure 5B), whereas levels of *Slc10a2* were elevated in ileum from *Gcgr*$^{-/-}$:*Glp2r*$^{+/+}$ but not in *Gcgr*$^{-/-}$:*Glp2r*$^{-/-}$ mice. Similarly, although levels of *Slc51b* and *Abcb11* were elevated in liver of *Gcgr*$^{-/-}$:*Gpbar1*$^{+/+}$ mice and *Slc10a2* was increased in ileum, no genotype-dependent differences in expression of these transcripts was detected in liver or ileum from *Gcgr*$^{-/-}$:*Gpbar1*$^{-/-}$ mice (Supplementary Figure 4)

The results of recent studies have demonstrated that the metabolic improvements arising following VSG are attenuated in *Nr1h4*$^{-/-}$ [23] and *Gpbar1*$^{-/-}$ mice [24], in a body weight-independent manner [25]. To determine whether the presence or absence of the *Glp2r* modifies key metabolic outcomes following bariatric surgery, we analyzed body weight and glucose control in high fat diet-fed *Glp2r*$^{+/+}$ vs. *Glp2r*$^{-/-}$ mice after VSG. Body weight, fat mass and lean mass were reduced to a similar extent in *Glp2r*$^{+/+}$ vs. *Glp2r*$^{-/-}$ mice (Figure 6A,B). Similarly, fasting glucose and both oral and intraperitoneal glucose tolerance were improved after VSG, but not different in *Glp2r*$^{+/+}$ vs. *Glp2r*$^{-/-}$ mice (Figure 6C).

4. DISCUSSION

The studies reported here were initiated in part to understand the potential relationship between and importance of the simultaneous elevations in BA and PGDPs observed in animal and human studies examining the metabolic consequences of genetic or pharmacological loss of GCGR signaling [7,8,11]. As BA are known to directly enhance PGDP secretion through TGR5, encoded by *Gpbar1*, localized to the basolateral surface of enteroendocrine L cells [17,18] it is plausible that increased levels of PGDPs may arise in part through the sustained activation of Gpbar1 on L cells. Nevertheless, *Gcgr*$^{-/-}$:*Gpbar1*$^{-/-}$ mice continue to exhibit improvements in glucose homeostasis and maintain increased circulating concentrations of GLP-1 at levels comparable to those detected in *Gcgr*$^{-/-}$ mice. These observations reveal that Gpbar1 is not critical for increased PGDP secretion or the principal metabolic phenotypes arising following genetic or pharmacological reduction of glucagon action. Furthermore, despite experimental evidence that BA independently promote intestinal growth [42], the increased bowel mass evident in *Gcgr*$^{-/-}$ mice was not diminished in *Gcgr*$^{-/-}$:*Gpbar1*$^{-/-}$ mice. It remains possible that some of the

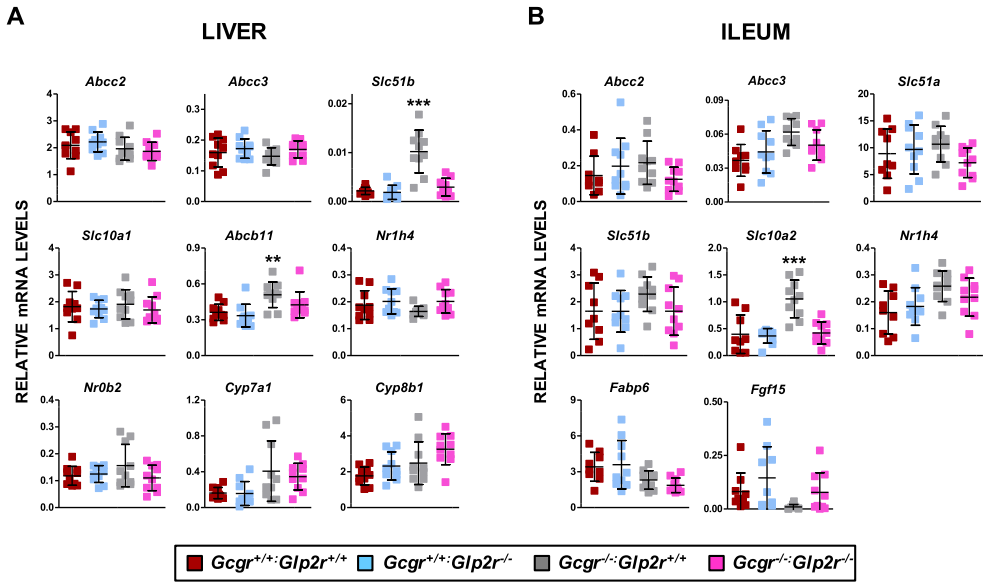

Figure 5: Expression of genes involved in bile acid metabolism in the liver (A) and ileum (B) of random-fed *Gcgr*$^{-/-}$*:Glp2r*$^{-/-}$ double knockout mice and their single knockout and wild-type littermates. mRNA levels of the indicated genes were assessed by real-time qPCR and normalized to *Ppia* and 18S rRNA levels in liver and ileum, respectively. Shown are individual data points with overlapping mean ± SD (n = 10 mice per genotype, combined from 2 independent mouse cohorts). Panels A & B: **p < 0.01 *Gcgr*$^{-/-}$*:Glp2r*$^{+/+}$vs *Gcgr*$^{+/+}$*:Glp2r*$^{+/+}$ & *Gcgr*$^{+/+}$*:Glp2r*$^{-/-}$; ***p < 0.001 *Gcgr*$^{-/-}$*:Glp2r*$^{+/+}$ vs *Gcgr*$^{+/+}$*:Glp2r*$^{+/+}$, *Gcgr*$^{+/+}$*:Glp2r*$^{-/-}$ & *Gcgr*$^{-/-}$*:Glp2r*$^{-/-}$. Statistical significance was assessed by one-way ANOVA followed by Bonferroni's multiple comparison post hoc test.

metabolic benefit ensuing from elevated BA in the context of diminished or extinguished glucagon action reflects signaling through FXR. Notably, both *Gpbar1*$^{-/-}$ and *Nr1h4*$^{-/-}$ mice exhibit independent reductions in acute nutrient-stimulated GLP-1 secretion [43]. Hence the putative independent contribution(s) of FXR to the *Gcgr*$^{-/-}$ phenotype and the actions of BAs on PGDP secretion in different experimental paradigms requires further study.

The examination of the role of GLP-2 in the phenotypes arising following loss of Gcgr signaling was prompted by observations in animals and humans that GLP-2 levels are increased following partial or complete attenuation of glucagon action [7,8,11]. Although studies of GLP-2 action are often focused on the gut mucosa, where it acts to expands enterocyte mass and augment nutrient absorption [6,44], complementary evidence supports a role for central GLP-2 action in the control of energy homeostasis and insulin action. Intracerebroventricular administration of GLP-2 inhibits food intake [45] through GLP-2R signaling within a subset of proopiomelanocortin (POMC) neurons [30]. The anorectic actions of exogenous GLP-2 were abolished in *Mcr4*$^{-/-}$ mice, whereas deletion of the *Glp2r* within POMC neurons produced hyperphagia and weight gain [30]. Furthermore, augmentation of central GLP-2 action suppressed hepatic glucose production and enhanced insulin sensitivity, favorable metabolic phenotypes overlapping with those reported in studies of *Gcgr*$^{-/-}$ mice [34,46]. Nevertheless, we did not detect differences in body weight, fasting glucose, or glucose tolerance in *Gcgr*$^{-/-}$*:Glp2r*$^{-/-}$ mice, relative to findings in *Gcgr*$^{-/-}$*:Glp2r*$^{+/+}$ mice, alone. Hence, the GLP-2R does not contribute to the major metabolic phenotypes arising from whole body loss of glucagon action in mice. In contrast, our findings confirm the importance of GLP-2R for the intestinal mucosal adaptation, including increased small bowel weight and length, that arises in *Gcgr*$^{-/-}$ mice [47]. These findings are consistent with a similar role for GLP-2R in the gut mucosa, actions arising secondarily to stimulation of crypt cell proliferation and increased crypt and villous depth of the small bowel epithelium [36,48].

Our experiments revealed a role for the GLP-2R in the elevation of circulating BAs in *Gcgr*$^{-/-}$ mice, as BA levels were lower in fed *Gcgr*$^{-/-}$*:Glp2r*$^{-/-}$ compared to *Gcgr*$^{-/-}$*:Glp2r*$^{+/+}$ mice. Moreover, the relative proportion of individual circulating BA is altered in *Gcgr*$^{-/-}$*:Glp2r*$^{-/-}$ mice. Understanding precisely how GLP-2 controls plasma BA levels will require further analysis; however, we did not detect compelling evidence for GLP-2R in control of ileal BA levels in *Gcgr*$^{-/-}$ mice. Infusion of GLP-2 in neonatal piglets maintained on parenteral nutrition increased liver bile acid content and upregulated hepatic expression of several bile export genes, as well as FXR [49]. GLP-2 also increased the expression of mRNA transcripts encoding the bile acid transport protein (*Fabp6*) in the distal small intestine of parenterally-fed rats [39]. Nevertheless, our previous analyses did not reveal an acute effect of GLP-2 on hepatic bile flow or ileal uptake and systemic appearance of taurocholic acid in mice [50]. Furthermore, our current studies reveal that with the exception of i) a reduction in the ileal expression of *Slc10a2* (encoding the apical sodium dependent bile acid transporter), and ii) decreased hepatic expression of *Slc51b* (encoding a basolateral bile acid transporter), loss of the *Glp2r* in the context of *Gcgr*$^{-/-}$ mice had little effect on BA-regulated gene expression in the intestine or liver. Hence the putative mechanisms linking GLP-2 action to the control of BA uptake, transport, or enterohepatic recirculation, and the corresponding reduction of circulating BA levels in *Gcgr*$^{-/-}$*:Glp2r*$^{-/-}$ mice, require further investigation.

Metabolic surgery represents a second intervention associated with increased plasma levels of BAs and PGDPs [21]. Indeed, there is considerable interest, based on results of preclinical studies of bariatric surgery in *Gpbar1*$^{-/-}$ [24,25] and *Nr1h4*$^{-/-}$ mice [23], in understanding the contributions of BAs to the mechanisms underlying improved glucose homeostasis and weight loss following experimental or clinical metabolic surgery. Similarly, plasma GLP-1 levels are often markedly increased after RYGB and increased, although to a lesser extent, after VSG [21]. These observations have fostered a vigorous debate surrounding the putative contribution(s) of

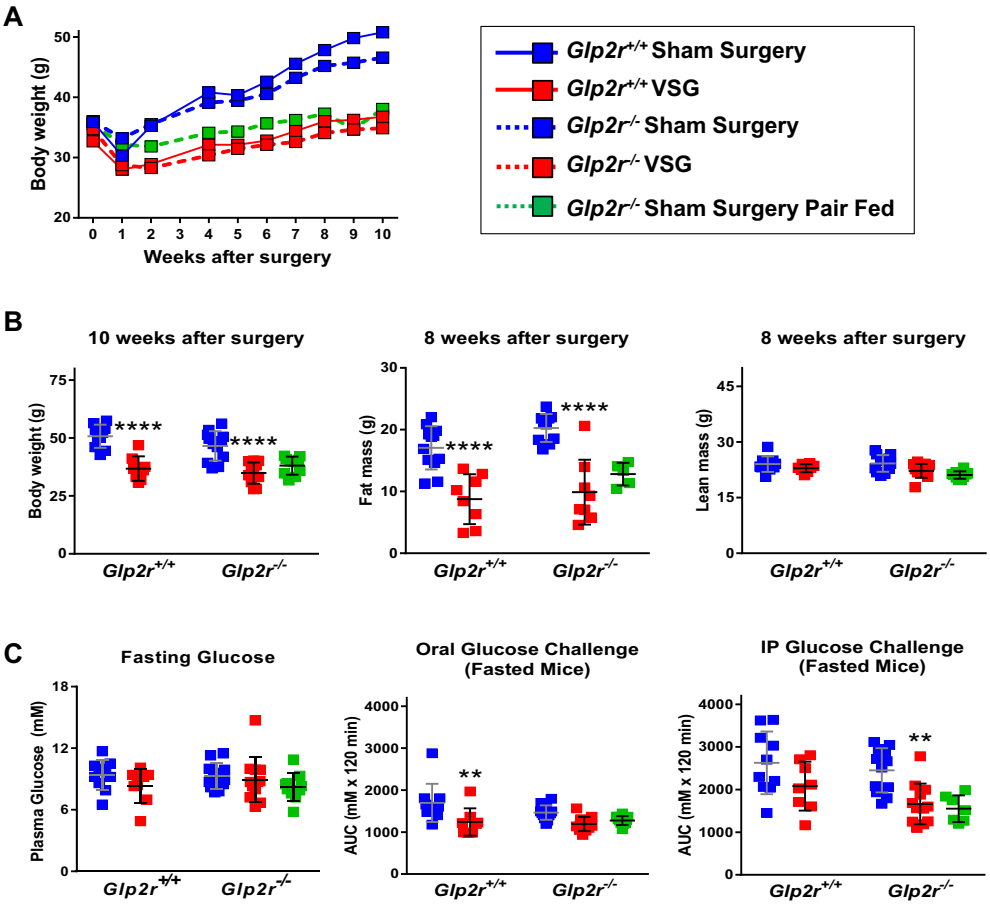

Figure 6: Body weight, body composition (A & B) and glucose tolerance (C) in *Glp2r* wild-type and knockout mice following vertical sleeve gastrectomy (VSG) surgery. Panel A: to facilitate body weight data visualization, only means without their associated error bars are shown. The coefficients of variation of the entire data set were $\geq$5.1% and $\leq$17.7% (n = 8–12 per group). Illustrated in panel B are individual data points with overlapping means ± SD (n = 8–12 mice per group, except n = 5 for Sham Surgery Pair Fed fat mass). Panel C: Glycemic excursion curves were delineated by measuring tail blood glycemia at 0, 15, 30, 45, 60 and 120 min after the specified glucose challenge, and glucose tolerance determined by calculating the corresponding AUCs. Shown are individual data points with overlapping mean ± SD (n = 8–12 mice per group). 2-way ANOVA indicated a not significant interaction term and also a not significant effect of VSG or genotype on "8 weeks after surgery lean mass" (panel B) and "fasting glucose" (panel C). In contrast, 2-way ANOVA indicated a not significant interaction term and a not significant effect of the genotype but a highly significant effect of VSG on "10 week after surgery body weight" ($F_{(1, 37)} = 56.79$, $p < 0.0001$), "8 weeks after surgery fat mass" ($F_{(1, 34)} = 56.11$, $p < 0.0001$) (panel B), "Oral Glucose Challenge AUC" ($F_{(1, 38)} = 15.84$, $p < 0.0003$) and "IP Glucose Challenge AUC" ($F_{(1, 38)} = 13.76$, $p < 0.0007$) (panel C). Panels B and C: **$p < 0.01$ & ****$p < 0.0001$ VSG vs Sham Surgery. The Sham Surgery Pair Fed group was not included in the statistical analysis.

GLP-1 action to the weight loss and improved glucose control evident following metabolic surgery [20–22]. Remarkably, although circulating GLP-2 levels are also considerably elevated after metabolic surgery [51], there has been little attention directed at examining whether GLP-2 receptor signaling contributes to the metabolic improvement after RYGB or VSG.

Our current studies reveal that the GLP-2R is not essential for reduction in glycemia and weight loss, arising after VSG in high fat-fed mice. These findings are surprising given data supporting a role for the GLP-2R in control of food intake, body weight and insulin sensitivity in mice [29,30,45,52]. Nevertheless, the lack of contribution of *Glp2r* to weight loss and reduced glycemia after VSG in mice is consistent with related findings demonstrating that the *Glp1r* is not required for the metabolic improvements arising after RYGB or VSG in high fat fed mice [27,53,54]. Hence, the hypothesis that elevated circulating levels of PGDPs, including GLP-2, contribute to the improvements in glucose control following glucagon receptor blockade, or metabolic surgery, is not substantiated by the current experimental evidence.

5. CONCLUSIONS AND LIMITATIONS

Our studies have a number of limitations. First, we studied BA biology and GLP-2 action in mice with germine mutations in the *Gcgr*, *Gpbar1*, and *Glp2r*, and the interpretation of our data may be complicated by unanticipated compensatory adaptations arising in mice with germline gene deletions. Second, $Gcgr^{-/-}$ mice are relatively resistant to development of diabetes and obesity [55]; hence, the data generated here in non-obese $Gcgr^{-/-}$ mice may not be relevant to findings obtained with transient Gcgr antagonism in more obese or diabetic mice or humans. Furthermore, although plasma levels of PGDPs, including GLP-2, are elevated in mice, rats and humans after VSG [20,21,51], it is possible that GLP-2 levels may be elevated to a greater extent, and the biology of GLP-2R may be more important, in experimental models analyzing the metabolic consequences of RYGB. Surprisingly, despite multiple reports linking GLP-2 to the control of appetite, glucose homeostasis, and insulin sensitivity, our data using two different experimental models characterized by increased levels of PGDPs failed to demonstrate a key role for the GLP-2R in regulation of glucose control or

body weight evident after disruption of Gcgr signaling, or following VSG. Similarly, despite the documented role for Gpbar1 for linking BA to control of PGDP secretion, plasma levels of circulating PGDPs were not different after loss of Gpbar1 in *Gcgr*$^{-/-}$ mice. Nevertheless, our findings reveal a role for the GLP-2R in a) gut adaptation b) the pathophysiological elevations of bile acids arising in fed *Gcgr*$^{-/-}$ mice and c) the relative proportions of circulating BA in *Gcgr*$^{-/-}$ mice, Our data, coupled with recent evidence linking GLP-2 to the control of gallbladder emptying [50], support the emergence of a GLP-2-BA axis, further expanding the complex relationship between BA, enteroendocrine cells, and the actions of the glucagon-like peptides.

DISCLOSURES

The authors report no relevant disclosures for these studies.

ACKNOWLEDGMENTS

DJD was supported in part by a foundation grant 154321 from the Canadian Institutes for Health Research, an investigator-initiated grant from Shire Pharmaceuticals, a Canada Research Chair in Regulatory Peptides, as well as a Banting and Best Diabetes Centre, Novo Nordisk Chair in Incretin Biology. The BA analysis reported in this study utilized Metabolomics Core Services supported by grant U24 DK097153 of NIH Common Funds Project to the University of Michigan.
DJD received consulting or speaking fees from Merck, Novo Nordisk Inc, and Pfizer Inc. DJD was a party, with University Health Network and University of Toronto, to a GLP-2 licensing agreement. RS received consulting or speaking fees from Ethicon Endo-Surgery/Johnson & Johnson Research, Orexigen, Novo Nordisk, Daiichi Sankyo, Novartis, Kallyope and Scohia.

CONFLICT OF INTEREST

None declared.

APPENDIX A. SUPPLEMENTARY DATA

Supplementary data related to this article can be found at https://doi.org/10.1016/j.molmet.2018.06.006.

REFERENCES

[1] Drucker, D.J., 2016. Evolving concepts and translational relevance of enteroendocrine cell biology. Journal of Clinical Endocrinology & Metabolism 101(3): 778–786.
[2] Gribble, F.M., Reimann, F., 2016. Enteroendocrine cells: chemosensors in the intestinal epithelium. Annual Review of Physiology, 78277–78299.
[3] Sandoval, D.A., D'Alessio, D.A., 2015. Physiology of proglucagon peptides: role of glucagon and GLP-1 in health and disease. Physiological Reviews 95(2): 513–548.
[4] Drucker, D.J., Habener, J.F., Holst, J.J., 2017. Discovery, characterization, and clinical development of the glucagon-like peptides. Journal of Clinical Investigation 127(12):4217–4227.
[5] Drucker, D.J., 2018. Mechanisms of action and therapeutic application of glucagon-like peptide-1. Cell Metabolism 27(4):740–756.
[6] Drucker, D.J., Yusta, B., 2014. Physiology and pharmacology of the enteroendocrine hormone glucagon-like peptide-2. Annual Review of Physiology, 76561–76583.
[7] Ali, S., Lamont, B.J., Charron, M.J., Drucker, D.J., 2011. Dual elimination of the glucagon and GLP-1 receptors in mice reveals plasticity in the incretin axis. Journal of Clinical Investigation 121(5):1917–1929.
[8] Kostic, A., King, T.A., Yang, F., Chan, K.C., Yancopoulos, G.D., Gromada, J., et al., 2018. A first-in-human pharmacodynamic and pharmacokinetic study of a fully human anti-glucagon receptor monoclonal antibody in normal healthy volunteers. Diabetes, Obesity and Metabolism 20(2):283–291.
[9] Yang, J., MacDougall, M.L., McDowell, M.T., Xi, L., Wei, R., Zavadoski, W.J., et al., 2011. Polyomic profiling reveals significant hepatic metabolic alterations in glucagon-receptor (GCGR) knockout mice: implications on anti-glucagon therapies for diabetes. BMC Genomics 12(1):281.
[10] Longuet, C., Robledo, A.M., Dean, E.D., Dai, C., Ali, S., McGuinness, I., et al., 2013. Liver-specific disruption of the murine glucagon receptor produces alpha-cell hyperplasia: evidence for a circulating alpha-cell growth factor. Diabetes 62(4):1196–1205.
[11] Guan, H.P., Yang, X., Lu, K., Wang, S.P., Castro-Perez, J.M., Previs, S., et al., 2015. Glucagon receptor antagonism induces increased cholesterol absorption. The Journal of Lipid Research 56(11):2183–2195.
[12] Borg, C.M., le Roux, C.W., Ghatei, M.A., Bloom, S.R., Patel, A.G., 2007. Biliopancreatic diversion in rats is associated with intestinal hypertrophy and with increased GLP-1, GLP-2 and PYY levels. Obesity Surgery 17(9): 1193–1198.
[13] Patti, M.E., Houten, S.M., Bianco, A.C., Bernier, R., Larsen, P.R., Holst, J.J., et al., 2009. Serum bile acids are higher in humans with prior gastric bypass: potential contribution to improved glucose and lipid metabolism. Obesity (Silver Spring) 17(9):1671–1677.
[14] Taqi, E., Wallace, L.E., de Heuvel, E., Chelikani, P.K., Zheng, H., Berthoud, H.R., et al., 2010. The influence of nutrients, biliary-pancreatic secretions, and systemic trophic hormones on intestinal adaptation in a Roux-en-Y bypass model. Journal of Pediatric Surgery 45(5):987–995.
[15] Romero, F., Nicolau, J., Flores, L., Casamitjana, R., Ibarzabal, A., Lacy, A., et al., 2012. Comparable early changes in gastrointestinal hormones after sleeve gastrectomy and Roux-En-Y gastric bypass surgery for morbidly obese type 2 diabetic subjects. Surgical Endoscopy 26(8):2231–2239.
[16] Cazzo, E., Pareja, J.C., Chaim, E.A., Geloneze, B., Barreto, M.R., Magro, D.O., 2017. GLP-1 and GLP-2 levels are correlated with satiety regulation after Roux-en-Y gastric bypass: results of an exploratory prospective study. Obesity Surgery 27(3):703–708.
[17] Thomas, C., Gioiello, A., Noriega, L., Strehle, A., Oury, J., Rizzo, G., et al., 2009. TGR5-mediated bile acid sensing controls glucose homeostasis. Cell Metabolism 10(3):167–177.
[18] Brighton, C.A., Rievaj, J., Kuhre, R.E., Glass, L.L., Schoonjans, K., Holst, J.J., et al., 2015. Bile acids trigger GLP-1 release predominantly by accessing basolaterally located G protein-coupled bile acid receptors. Endocrinology 156(11):3961–3970.
[19] Nielsen, S., Svane, M.S., Kuhre, R.E., Clausen, T.R., Kristiansen, V.B., Rehfeld, J.F., et al., 2017. Chenodeoxycholic acid stimulates glucagon-like peptide-1 secretion in patients after Roux-en-Y gastric bypass. Physiological Reports 5(3).
[20] Hutch, C.R., Sandoval, D., 2017. The role of GLP-1 in the metabolic success of bariatric surgery. Endocrinology 158(12):4139–4151.
[21] Madsbad, S., Dirksen, C., Holst, J.J., 2014. Mechanisms of changes in glucose metabolism and bodyweight after bariatric surgery. The Lancet Diabetes and Endocrinology 2(2):152–164.
[22] Mulla, C.M., Middelbeek, R.J.W., Patti, M.E., 2018. Mechanisms of weight loss and improved metabolism following bariatric surgery. Annals of the New York Academy of Sciences 1411(1):53–64.
[23] Ryan, K.K., Tremaroli, V., Clemmensen, C., Kovatcheva-Datchary, P., Myronovych, A., Karns, R., et al., 2014. FXR is a molecular target for the effects of vertical sleeve gastrectomy. Nature 509(7499):183–188.
[24] Ding, L., Sousa, K.M., Jin, L., Dong, B., Kim, B.W., Ramirez, R., et al., 2016. Vertical sleeve gastrectomy activates GPBAR-1/TGR5 to sustain weight loss, improve fatty liver, and remit insulin resistance in mice. Hepatology 64(3): 760–773.

[25] McGavigan, A.K., Garibay, D., Henseler, Z.M., Chen, J., Bettaieb, A., Haj, F.G., et al., 2017. TGR5 contributes to glucoregulatory improvements after vertical sleeve gastrectomy in mice. Gut 66(2):226–234.

[26] Garibay, D., McGavigan, A.K., Lee, S.A., Ficorilli, J.V., Cox, A.L., Michael, M.D., et al., 2016. Beta-cell glucagon-like Peptide-1 receptor contributes to improved glucose tolerance after vertical sleeve gastrectomy. Endocrinology 157(9):3405–3409.

[27] Wilson-Pérez, H.E., Chambers, A.P., Ryan, K.K., Li, B., Sandoval, D.A., Stoffers, D., et al., 2013. Vertical sleeve gastrectomy is effective in two genetic mouse models of glucagon-like peptide-1 receptor deficiency. Diabetes 62(7): 2380–2385.

[28] Banasch, M., Bulut, K., Hagemann, D., Schrader, H., Holst, J.J., Schmidt, W.E., et al., 2006. Glucagon-like peptide 2 inhibits ghrelin secretion in humans. Regulatory Peptides 137(3):173–178.

[29] Shi, X., Zhou, F., Li, X., Chang, B., Li, D., Wang, Y., et al., 2013. Central GLP-2 enhances hepatic insulin sensitivity via activating PI3K signaling in POMC neurons. Cell Metabolism 18(1):86–98.

[30] Guan, X., Shi, X., Li, X., Chang, B., Wang, Y., Li, D.P., et al., 2012. GLP-2 receptor in POMC neurons suppresses feeding behavior and gastric motility. American Journal of Physiology Endocrinology and Metabolism 130(7):E853–E864.

[31] Cani, P.D., Possemiers, S., Van de Wiele, T., Guiot, Y., Everard, A., Rottier, O., et al., 2009. Changes in gut microbiota control inflammation in obese mice through a mechanism involving GLP-2-driven improvement of gut permeability. Gut 58(8):1091–1103.

[32] Monte, S.V., Caruana, J.A., Ghanim, H., Sia, C.L., Korzeniewski, K., Schentag, J.J., et al., 2012. Reduction in endotoxemia, oxidative and inflammatory stress, and insulin resistance after Roux-en-Y gastric bypass surgery in patients with morbid obesity and type 2 diabetes mellitus. Surgery 151(4):587–593.

[33] Kelly, A.S., Ryder, J.R., Marlatt, K.L., Rudser, K.D., Jenkins, T., Inge, T.H., 2016. Changes in inflammation, oxidative stress and adipokines following bariatric surgery among adolescents with severe obesity. International Journal of Obesity (London) 40(2):275–280.

[34] Gelling, R.W., Du, X.Q., Dichmann, D.S., Romer, J., Huang, H., Cui, L., et al., 2003. Lower blood glucose, hyperglucagonemia, and pancreatic {alpha} cell hyperplasia in glucagon receptor knockout mice. Proceedings of the National Academy of Sciences of the U S A, 1001438–1001443.

[35] Vassileva, G., Golovko, A., Markowitz, L., Abbondanzo, S.J., Zeng, M., Yang, S., et al., 2006. Targeted deletion of Gpbar1 protects mice from cholesterol gallstone formation. Biochemical Journal 398(3):423–430.

[36] Lee, S.-J., Lee, J., Li, K.K., Holland, D., Maughan, H., Guttman, D.S., et al., 2012. Disruption of the murine Glp2r impairs Paneth cell function and increases susceptibility to small bowel enteritis. Endocrinology 153(3): 1141–1151.

[37] Chambers, A.P., Kirchner, H., Wilson-Perez, H.E., Willency, J.A., Hale, J.E., Gaylinn, B.D., et al., 2013. The effects of vertical sleeve gastrectomy in rodents are ghrelin independent. Gastroenterology 144(1):50–52 e55.

[38] Griffiths, W.J., Sjovall, J., 2010. Bile acids: analysis in biological fluids and tissues. The Journal of Lipid Research 51(1):23–41.

[39] Kitchen, P.A., Goodlad, R.A., FitzGerald, A.J., Mandir, N., Ghatei, M.A., Bloom, S.R., et al., 2005. Intestinal growth in parenterally-fed rats induced by the combined effects of glucagon-like peptide 2 and epidermal growth factor. JPEN – Journal of Parenteral and Enteral Nutrition 29(4):248–254.

[40] Lim, D.W., Wales, P.W., Josephson, J.K., Nation, P.N., Wizzard, P.R., Sergi, C.M., et al., 2016. Glucagon-like peptide 2 improves cholestasis in parenteral nutrition–associated liver disease. JPEN – Journal of Parenteral and Enteral Nutrition 40(1):14–21.

[41] Conarello, S.L., Jiang, G., Mu, J., Li, Z., Woods, J., Zycband, E., et al., 2007. Glucagon receptor knockout mice are resistant to diet-induced obesity and streptozotocin-mediated beta cell loss and hyperglycaemia. Diabetologia 50(1):142–150.

[42] Dossa, A.Y., Escobar, O., Golden, J., Frey, M.R., Ford, H.R., Gayer, C.P., 2016. Bile acids regulate intestinal cell proliferation by modulating EGFR and FXR signaling. American Journal of Physiology – Gastrointestinal and Liver Physiology 310(2):G81–G92.

[43] Pathak, P., Liu, H., Boehme, S., Xie, C., Krausz, K.W., Gonzalez, F., et al., 2017. Farnesoid X receptor induces Takeda G-protein receptor 5 cross-talk to regulate bile acid synthesis and hepatic metabolism. Journal of Biological Chemistry 292(26):11055–11069.

[44] Drucker, D.J., Ehrlich, P., Asa, S.L., Brubaker, P.L., 1996. Induction of intestinal epithelial proliferation by glucagon-like peptide 2. Proceedings of the National Academy of Sciences of the U S A, 937911–937916.

[45] Tang-Christensen, M., Larsen, P.J., Thulesen, J., Romer, J., Vrang, N., 2000. The proglucagon-derived peptide, glucagon-like peptide-2, is a neurotransmitter involved in the regulation of food intake. Nature Medicine 6(7):802–807.

[46] Sorensen, H., Winzell, M.S., Brand, C.L., Fosgerau, K., Gelling, R.W., Nishimura, E., et al., 2006. Glucagon receptor knockout mice display increased insulin sensitivity and impaired {beta}-Cell function. Diabetes 55(12): 3463–3469.

[47] Koehler, J.A., Baggio, L.L., Yusta, B., Longuet, C., Rowland, K.J., Cao, X., et al., 2015. GLP-1R agonists promote normal and neoplastic intestinal growth through mechanisms requiring Fgf7. Cell Metabolism 21(3):379–391.

[48] Wismann, P., Barkholt, P., Secher, T., Vrang, N., Hansen, H.B., Jeppesen, P.B., et al., 2017. The endogenous preproglucagon system is not essential for gut growth homeostasis in mice. Molecular Metabolism 6(7):681–692.

[49] Lim, D.W., Wales, P.W., Mi, S., Yap, J.Y., Curtis, J.M., Mager, D.R., et al., 2016. Glucagon-like Peptide-2 alters bile acid metabolism in parenteral nutrition–associated liver disease. JPEN – Journal of Parenteral and Enteral Nutrition 40(1):22–35.

[50] Yusta, B., Matthews, D., Flock, G.B., Ussher, J.R., Lavoie, B., Mawe, G.M., et al., 2017. Glucagon-like peptide-2 promotes gallbladder refilling via a TGR5-independent, GLP-2R-dependent pathway. Molecular Metabolism 6(6):503–511.

[51] Cazzo, E., Gestic, M.A., Utrini, M.P., Chaim, F.D., Geloneze, B., Pareja, J.C., et al., 2016. Glp-2: a poorly understood mediator enrolled in various bariatric/metabolic surgery-related pathophysiologic mechanisms. Arquivos Brasileiros de Cirurgia Digestiva 29(4):272–275.

[52] Baldassano, S., Rappa, F., Amato, A., Cappello, F., Mule, F., 2015. GLP-2 as beneficial factor in the glucose homeostasis in mice fed a high fat diet. Journal of Cellular Physiology 230(12):3029–3036.

[53] Ye, J., Hao, Z., Mumphrey, M.B., Townsend, R.L., Patterson, L.M., Stylopoulos, N., et al., 2014. GLP-1 receptor signaling is not required for reduced body weight after RYGB in rodents. American Journal of Physiology – Regulatory, Integrative and Comparative Physiology 306(5):R352–R362.

[54] Mokadem, M., Zechner, J.F., Margolskee, R.F., Drucker, D.J., Aguirre, V., 2014. Effects of Roux-en-Y gastric bypass on energy and glucose homeostasis are preserved in two mouse models of functional glucagon-like peptide-1 deficiency. Molecular Metabolism 3(2):191–201.

[55] Campbell, J.E., Drucker, D.J., 2015. Islet alpha cells and glucagon–critical regulators of energy homeostasis. Nature Reviews Endocrinology 11(6): 329–338.

